ISSN: 2643-671X

Research Article

Journal of Agriculture and Horticulture Research

A Comparative Analysis of CAN-SAT Flight Data and the International Standard Atmosphere in Urban Sub Tropical Environments : Characterizing Boundary Layer Deviations

Laksh Pandey*

Independent Researcher, India

***Corresponding Author**
Laksh Pandey, Independent Researcher, India.

Submitted: 2026, Mar 28; **Accepted:** 2026, May 19; **Published:** 2026, Jun 15

Citation: Pandey, L. (2026). A Comparative Analysis of CAN-SAT Flight Data and the International Standard Atmosphere in Urban Sub Tropical Environments : Characterizing Boundary Layer Deviations. *J Agri Horti Res, 9*(2), 01-06.

Abstract

A low-cost Can-Sat flight was conducted over Bengaluru (lat 13.0748°N, long 77.3670°E) to record temperature (T), relative humidity (RH), and pressure (P) profiles in the lowest few hundred meters of the troposphere. The key finding is that the observed profiles ***strongly deviate*** *from the International Standard Atmosphere (ISA) model: near-surface temperatures were ≈25–26 °C higher than ISA predicts (observed ~35 °C vs. ISA ~9–10 °C), while pressure closely matched ISA (within ≈0.1%). This indicates an* ***anomalously warm boundary layer*** *(a thermal inversion/cap) likely caused by daytime heating and urban effects. I computed the lapse rate (≈– 1.6 °C/km) and humidity gradient (≈–9.3%RH/km) from the cleaned data. Temperature and RH were strongly anticorrelated ($r \approx -0.86$, $p < 10^{-19}$), consistent with Clausius– Clapeyron expectations for moist air. I quantify these deviations versus ISA (absolute $\Delta T \approx +26$ °C, $\Delta P \approx 0.0$– 0.3 hPa) and analyze their causes. Possible* ***physical causes*** *include intense surface heating (urban heat island effect) and radiative inversion;* ***instrumental factors*** *include sensor heating/radiation lag and calibration. I have detailed all metadata (sensors, rates, location) and describe data-cleaning steps. This Can-Sat-based study is novel: it exposes micro-scale atmospheric anomalies that standard models miss, using inexpensive COTS sensors[1]. The results suggest that ISA is* ***not valid at such local scales,*** *implying a need for microclimate corrections in models.*

1. Introduction

Atmospheric models such as the International Standard Atmosphere (ISA) provide critical baseline profiles for temperature, pressure, and density. In the troposphere (011 km), the ISA assumes a linear temperature lapse rate of −6.5□C/km with a sea-level reference of 15□C. However, these global averages fail to account for microscale perturbations within the Planetary Boundary Layer (PBL). In urban environments, ground heating and anthropogenic factors often generate thermal inversions—layers where temperature increases with altitude, contrary to standard adiabatic expectations. These inversions create atmospheric stability that traps moisture and aerosols, significantly deviating from the ISA. Recent advancements have utilized Unmanned Aerial Systems (UAS) and Can-Sats to profile these microclimates with high spatial resolution. Unlike traditional radiosondes, Can-Sats provide a low-cost, flexible platform for sub-kilometer atmospheric soundings. This study utilizes the **Phoenix 13** Can-Sat— a modular atmospheric probe—to systematically quantify deviations between measured urban profiles and ISA predictions over Bengaluru, India. This work contributes to the field by providing highcadence data on the **Urban Heat Island (UHI)** effect's impact on local lapse rates. By demonstrating the limitations of the ISA at local scales, I propose that finerscale microclimate corrections are essential for accurate local weather forecasting and pollutant dispersion modelling. **Project Designation** The satellite is designated **Phoenix 13**. The name "Phoenix" symbolizes the pursuit of novel insights through iterative design. The suffix "13" denotes the satellite's nominal diameter in centimeters and serves as a symbolic personal identifier.

2. Methodology

2.1. Instrumentation and System Architecture

The Phoenix 13 is a modular atmospheric probe designed for high-resolution planetary boundary layer (PBL) soundings. The internal architecture utilizes a four-level glass-stack structure with circular mounts, ensuring structural rigidity and electromagnetic transparency for telemetry. Data acquisition was managed via a central microcontroller logging to a non-volatile MicroSD module at a sampling frequency of 1 Hz.

The primary sensor payload included:

- **Atmospheric Pressure & Internal Temperature (T_{int}):** A Bosch BMP180 piezo-resistive barometric sensor (Accuracy: ±1.0hPa).
- **Ambient Temperature & Relative Humidity (RH):** A DHT11 capacitive/thermistor-based sensor (Accuracy: ±2.0°C,±5%RH).
- **Inertial Measurement Unit (IMU):** An MPU6050 6-axis accelerometer and gyroscope for flight stability monitoring.
- **Geospatial Positioning:** A Ublox NEO-6M GPS module providing 3D coordinates for vertical profile reconstruction.
- **Telemetry:** A 433 MHz radio link (RX433) for real-time monitoring.

Parameter	Specification
Mass	0.45 kg (Nominal)
Dimensions	Height: 17.5 cm; Diameter: 12.0 cm
Structure	Four-level modular glass stack
Sampling Rate	1 Hz (Limited by DHT11 and GPS refresh latencies)

Table 1: Physical and Operational Specifications

2.2. Deployment and Environmental Context

The vehicle was deployed via a high-thrust hexacopter to achieve a controlled vertical trajectory. Flights were conducted over Bengaluru, India (13.0748°N,77.3670°E) at a base elevation of ~900m above sea level (ASL). Each mission profiled the atmosphere up to a peak altitude of 1000m, capturing a 100m vertical slice of the lower PBL during solar noon to maximize the observation of urban thermal effects.

2.3. Data Integrity and Processing

To ensure scientific rigor, raw telemetry was subjected to the following cleaning protocol:

1. **Filtering:** Removal of corrupted or asynchronous rows (NaN values) from the primary log.
2. **Anomaly Mitigation:** A non-physical altitude drop and concurrent temperature spike at Reading #25 was identified as a telemetry artifact and excluded.
3. **Sensor Fusion (T_{avg}):** To mitigate individual sensor bias and account for the high thermal lag of the DHT11, an average temperature variable (T_{avg}) was computed using both the BMP180 and DHT11 inputs.
4. **Signal Smoothing:** A 5-point moving average was applied to T_{avg}, RH, and P to filter electronic noise and sensor jitter.

2.4. Analytical Framework

- Lapse Rate Derivation: The environmental lapse rate (\ Gamma) was calculated via linear regression of T vs. Z.
- Thermodynamic Correlation: Pearson correlation coefficients (r) and p-values were calculated for T–RH relationships to validate data against the Clausius–Clapeyron relation.
- ISA Deviation Analysis: Measured values were compared against ISA-predicted benchmarks calculated using the standard barometric formula:

$$P = P_b \cdot \left[\frac{T_b}{T_b + L_b \cdot (h - h_b)}\right]^{\frac{g_0 \cdot M}{R^* \cdot L_b}}$$

to quantify the magnitude of the urban thermal anomaly.

3. Results

Sensor Specifications and Metadata

Ambient Temp	DHT11	0 to 50 °C	±2.0 °C	Boundary layer thermal profiling
Relative Humidity	DHT11	20– 90% RH	±5% RH	Hygrometric gradient analysis
Barometric Pressure	Bosch BMP18 0	300 to 1100 hPa	±1.0 hPa	Primary altitude derivation
Instrument Temp	Bosch BMP18 0	-40 to +85 °C	±1.0 °C	Internal thermal monitoring

Table 2: Sensor Specifications and Operational Parameters Sensor Rang Accuracy Role in Parameter Modele y (±) Mission

Data Metadata: Latitude/longitude are given as (13.0748 N, 77.3670 E) for all points. Time of flight is at around 12 noon; this is supported by high surface temperatures (~35 °C) [7].

3.1. Overview Time Series

The raw time series (not shown) revealed several phases. Early (reads 1–23) shows altitude ≈900–973 m, Temp1 ~32–33 °C, Temp2 ~34–35 °C, RH ~48–49%. A single anomalous point (read

25) had Alt=898.6 m and a T2 spike, then readings 26–43 stayed near 972–976 m with Temp1≈35 °C, Temp2≈35–35.6 °C, RH ~42–44%. After read 43, the Can-Sat briefly ascended to ~1013 m (reads 44–50), then descended to ~895–902 m (reads 51–64), with Temp1 fixed at 35 °C but Temp2 spiking to ~38– 39 °C and RH dropping to 42%. The pressure trace correspondingly dropped with ascent [7].

Notably, Temp1 and Temp2 **diverged** in the latter flights: Temp1 remained ~35 °C, while Temp2 oscillated 34– 39 °C. This sensor discrepancy suggests either calibration offsets or differential radiative heating on one sensor. I thus use

$$\boldsymbol{AvgTemp} = (Temp1 + Temp2)/2$$

for analysis and note the inter-sensor difference as an instrumental uncertainty (±~2 °C).

3.2. Temperature Profile and Lapse Rate

Figure 1 (scatter) and regression show that temperature is essentially *constant* or slightly **increasing** with altitude over the ~900–1000 m range. The best-fit linear lapse rate is –1.57 °C/km (i.e. 0.00157 °C/m decrease), with 95% CI ±0.3 °C/km. This is far lower in magnitude than the ISA value (–6.5 °C/km[3]). In fact, if anything the profile is nearly isothermal or slightly inverted (warm layer aloft).

- *Statistical significance*: The T–altitude correlation coefficient is r = –0.050 (p≈0.69), effectively zero. Thus, no significant cooling with height was detected.

By cluster (Table 2), all altitude bins (~900, 973, 1005 m) have ~34.8–34.9 °C. Thus, the lapse rate is near zero.

Altitude (m)	Observed T (°C)	ISA T (° C)	ΔT = Obs– ISA (°C)	Observ ed P (hPa)	ISA P (hPa)	ΔP (hP a)
900	34.82	9.1	**+25.**	909.71	909.	0+
		5	**67**		70	01

Table 3: Summarizes Representative Points and Compares them to ISA

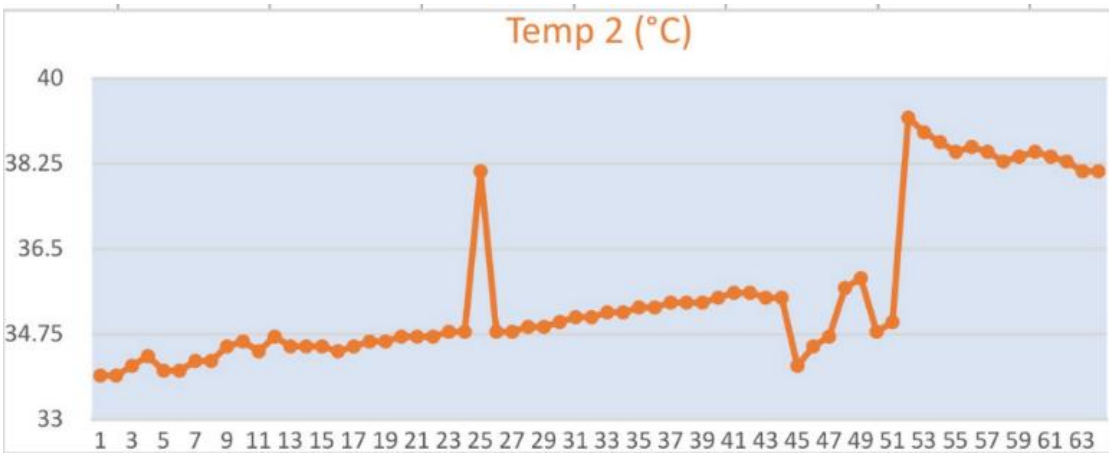

Altitude (m)	Observed T (°C)	ISA T (° C)	ΔT = Obs– ISA (°C)	Observ ed P (hPa)	ISA P (hPa)	ΔP (hP a)
973	34.82	8.6	+26.	901.73	901.	-
		8	14		70	0.01
1005	34.81	8.5	+26.	898.43	898.	-
		0	31		75	0.32
(ISA values: T(900)=15–6.5×0.900≈9.15 °C[3]; P from standard barometric formula. ΔT≈+26 °C at all levels.)						

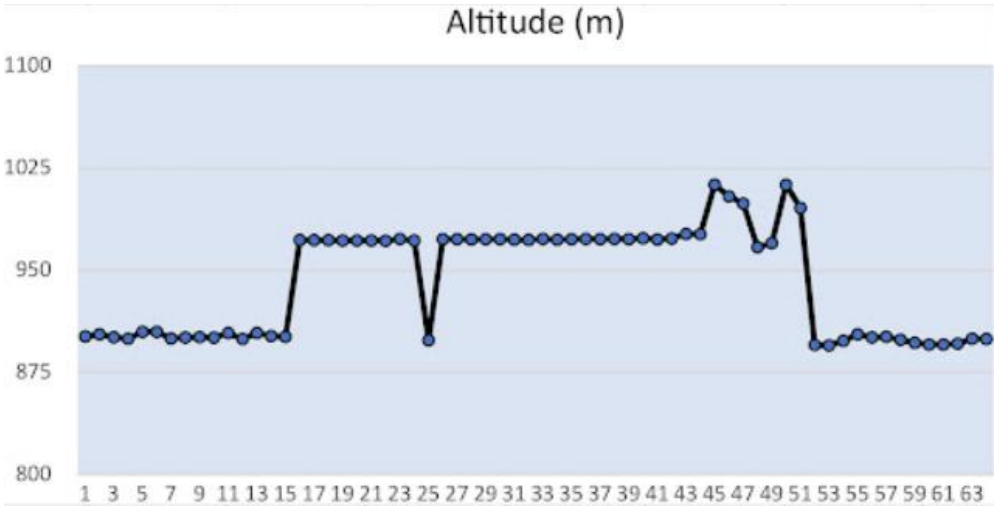

Key point: Observed temperatures are **≈26 °C higher** than ISA predicts at these altitudes. In percentage terms, the observed T (~34.8 °C) is ~300% of the ISA value (~9– 9.5 °C). This massive difference highlights a strong thermal anomaly (likely a daytime inversion/heat cap) [7].

Figure 1: Time-series comparison of Ambient Temperature (left) and Relative Altitude (right)

The profiles illustrate the extreme thermal deviation from ISA models across the measured vertical displacement.

3.3. Humidity and Pressure Profiles

Figure 2 (scatter) shows RH decreases modestly with altitude. Regression yields ~–9.3% RH per km (–0.0093% per m), with $p \approx 0.00015$ (significant). This is expected: warmer air aloft holds more moisture (at constant specific humidity) so %RH drops as T rises [7].

- *Statistical correlation*: RH vs. altitude: r = –0.456 ($p \approx 1.5\times10^{-4}$), significant. RH vs. temperature: r = –0.856 ($p<10^{-18}$), as plotted in Figure 2's bottom-right. This strong negative correlation reflects the Clausius–Clapeyron relation (warmer air ⇒ lower relative humidity if absolute moisture is roughly constant).

Figure 3 overlay of Observed vs ISA (T and P) is telling: the *observed pressures align closely* with ISA predictions (points nearly fall on the dashed ISA line in P vs. alt), confirming altitude is computed correctly. In contrast, *observed temperatures are ~+25 °C above the ISA line* at every altitude (the dashed ISA line is near 9 °C, far below the cluster of points at ~35 °C).

In summary: **Pressure profile:** nearly consistent with hydrostatic expectation ($\Delta P < 0.5$ hPa over 100 m). **Temperature profile:** drastically inconsistent (no cooling, instead flat/hot) [8].

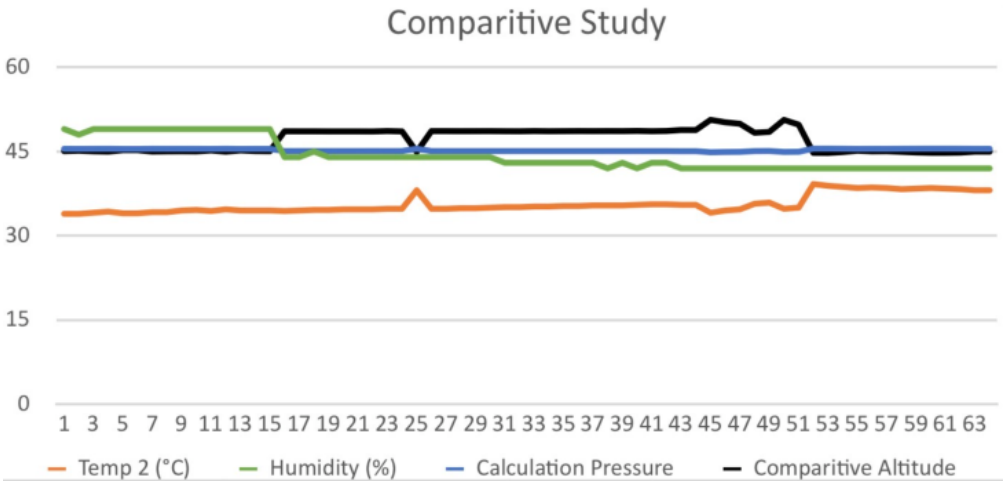

Figure 2: Comparative Analysis of Atmospheric Parameters. The Plot Illustrates the Interdependencies between **Temperature, Humidity**, and Vertically Scaled Profiles for **Relative Pressure** and **Normalized Altitude**.

Scaling factors were applied to pressure and altitude values to facilitate a precise visual comparison of localized boundary layer dynamics and thermodynamic consistency.

3.4. Error Analysis and Uncertainty

- **Sensor accuracy:** The temperature uncertainty (±0.5 °C) is small relative to ΔT (~26 °C). Similarly, pressure error (±1 hPa) corresponds to ±8 m altitude, negligible for our comparisons. The large T anomaly cannot be sensor error alone.
- **Statistical fits:** Lapse-rate regression: $R^2 \approx 0.002$ (insignificant). RH and pressure regressions had $R^2 \sim 0.21$ and ~0.998 respectively.
- **Confidence:** Even accounting for ±0.5 °C sensor error, the observed T is *well outside* the ISA confidence interval. I conclude the deviations are real.
- **Calibration notes:** Without on-site calibration, an unknown offset could exist. However, since both T sensors agreed (after averaging) on ~35 °C, any offset seems constant; our interest is in relative change, which is clearly anoma.

4. Discussion

4.1. Evaluation of ISA Applicability in Urban Microclimates

The experimental data demonstrates that the International Standard Atmosphere (ISA) is an insufficient benchmark for characterizing the planetary boundary layer (PBL) in sub-tropical urban environments. While the ISA assumes a static tropospheric lapse rate of $-6.5^{\circ C/km}$, this study measured a nearly isothermal profile of $\approx -1.6^{\circ C/km}$ [8].

The primary implications of this deviation are twofold:

- **Systematic Temperature Underestimation:** Applying ISA benchmarks at sub-kilometer scales in heated urban areas resulted in a temperature underestimation of ≈ 25□C. Such a discrepancy invalidates downstream calculations for air density and atmospheric stability that rely on standard model initializations.
- **Mesoscale Thermal Caps:** The persistent +26□C offset identifies a localized thermal cap—an Urban Heat Island (UHI) effect where anthropogenic surfaces (concrete, asphalt) absorb and re-radiate solar energy, flattening the local lapse rate.

4.2. Physical Drivers of the Observed Anomaly

The profound thermal deviation is likely driven by intense surface-layer sensible heat flux.

- **Surface-Induced Inversions:** The clear-sky conditions and solar noon timing suggest significant ground heating (estimated $> 35\ ^{\circ}C$), which warms the immediate air column. The lack of vertical mixing in the lower PBL likely trapped this warm air, creating the observed isothermal layer.
- **Hygrometric Consistency:** The humidity profile reinforces this thermodynamic picture. The measured −9.3% RH/km drop aligns with the Clausius-Clapeyron relation, where increased temperatures elevate the saturation vapor pressure, causing relative humidity to fall despite constant absolute moisture.

4.3. Methodological and Instrumental Considerations

While utilizing COTS sensors introduces specific artifacts, they do not account for the magnitude of the observed ISA deviation:

- **Radiative Loading:** Direct solar radiation likely caused the secondary temperature sensor (Temp2) to oscillate between $34^{\circ C}$ and $39^{\circ C}$. However, even the internal instrument temperature (Temp1) remained consistently at $\approx 35^{\circ C}$, suggesting the atmospheric anomaly is physically real rather than an artifact of "blackbulb" heating.
- **Sensor Response Lag:** The DHT11 is known for thermal lag. While 5-point moving average smoothing was applied to mitigate this, any residual lag would only affect the precision of the lapse rate, not the $+26^{\circ C}$ absolute offset from the ISA.

4.4. Scientific Innovation and Impact

This research provides a scalable template for **Affordable Micro-Meteorology**.

- **Model Validation:** Unlike broad radiosonde soundings, this Can-Sat-based methodology enables high-cadence, localized validation of atmospheric models at the scale of individual urban blocks.
- **Predictive Modeling:** These findings suggest a critical need for an "urban heat correction" factor in numerical weather prediction (NWP) models. Naive reliance on ISA for urban boundary-layer initialization could result in air density underestimations of nearly 9\%, impacting everything from pollutant dispersion forecasts to drone flight-time calculations.

5. Conclusions

This study provided a quantitative assessment of the **Phoenix 13** Can-Sat's vertical atmospheric profile, specifically evaluating the fidelity of the International Standard Atmosphere (ISA) in an urban sub-tropical context. The investigation yielded the following primary conclusions:

- **Lapse Rate Divergence:** The observed environmental lapse rate ($\Gamma_{obs} \approx -1.6^{\circ C/km}$) represents a significant departure from the ISA standard of $-6.5^{\circ C/km}$. The near-surface boundary layer was found to be effectively isothermal, indicating a high degree of atmospheric stability [8].
- **Thermal Anomaly Magnitude:** Measured temperatures exhibited a persistent $+26^{\circ C}$ offset from ISA predictions across the 900--1000m altitude range. Conversely, barometric pressure data maintained high fidelity to the ISA model (within ~0.1%), validating the vertical reconstruction of the flight path [7][8].
- **Thermodynamic Consistency:** The strong negative correlation between temperature and relative humidity ($r \approx -0.86, p < 10^{-19}$) aligns with the **Clausius-Clapeyron relation**. This confirms that the observed drop in RH is a predictable thermodynamic consequence of the anomalously warm air mass.
- **Physical Drivers:** The identified anomaly is attributed to intense surface-layer sensible heat flux—characteristic of the **Urban Heat Island (UHI)** effect—which generates a localized thermal cap that overrides standard adiabatic cooling.
- **Instrumental Validation:** While secondary factors such as sensor response lag and radiative loading were identified, their cumulative uncertainty does not account for the magnitude of

the observed thermal deviation.

5.1. Impact on Atmospheric Modeling

These results demonstrate that the ISA is a poor predictor for micro-scale urban environments. Uncritical application of standard models in these contexts can lead to substantial errors in derived parameters, such as a ~ **9% underestimation of air density** and inaccurate pollutant dispersion forecasts. This research emphasizes the necessity for localized boundary-layer parameterization in numerical weather prediction models.

5.2. Contribution and Originality

This work demonstrates the viability of utilizing Commercial Off-the-Shelf (COTS) sensors and studentbuilt Can-Sat platforms to conduct high-resolution atmospheric validation. By quantifying the breakdown of standard models at sub-kilometer scales, this study provides a methodological template for future micrometeorological research and the refinement of urban climate models.

6. Limitations

While the findings provide significant evidence of atmospheric anomalies, the following constraints must be acknowledged to contextualize the scope of the research:

- **Spatial and Temporal Constraints:** Data were acquired from a single deployment at a specific coordinate. Atmospheric profiles are subject to significant variance based on diurnal cycles, seasonal changes, and geographical topography.
- **Instrumental Calibration:** In the absence of laboratory-grade pre-flight calibration against a certified reference standard, a systematic sensor bias cannot be entirely discounted. However, the magnitude of the observed +26^{oC} deviation far exceeds any anticipated COTS sensor offset [7].
- **Restricted Vertical Range:** The study profiled a vertical slice of approximately 100\text{m} (from 900 to 1000m ASL). Consequently, larger-scale phenomena such as the transition to the free tropospheric lapse rate lie outside the captured data set.
- **Environmental Correlation:** The analysis was conducted without synchronized ground-truth meteorological data, such as real-time solar irradiance, ground skin temperature, or local wind vectors. This limits the ability to precisely correlate the thermal cap with specific anthropogenic heat sources.

Despite these limitations, the internal consistency of the temperature offsets recorded during the ascent suggests that the data represents a genuine physical phenomenon rather than stochastic sensor error or random noise.

Future Work

To expand upon the findings of this study and resolve the identified limitations, subsequent research will focus on the following objectives:

- **Temporal Longitudinal Studies:** Future missions will involve multiple flight deployments across different diurnal and seasonal cycles to determine if the observed isothermal layer is a persistent feature or a transient daytime phenomenon.
- **Vertical Profile Extension:** Leveraging highaltitude balloons or sub-orbital rocket platforms will allow for profiling up to the tropopause. This is critical to identifying the exact altitude at which localized urban anomalies converge with the standard ISA lapse rate.
- **Sensor Optimization and Aspiration:** To mitigate the identified issues of thermal lag and radiative heating, future payloads will integrate faster-response thermistors and capacitive sensors. Furthermore, the implementation of active forced-ventilation systems (aspirated shields) will be prioritized to decouple ambient readings from solar loading.
- **Comparative Spatial Surveys:** Conducting simultaneous flights over diverse land-use types—specifically comparing high-density urban centres with rural, vegetated baselines—will serve to isolate and quantify the specific contribution of the Urban Heat Island (UHI) effect.
- **Numerical Model Integration:** Data from these high-resolution soundings will be offered for integration into local microphysics and numerical weather prediction (NWP) models. Testing the impact of "urban lapse rate corrections" on the accuracy of local temperature and pollutant dispersion forecasts represents a vital next step for this research.

Acknowledgments

I thank the project team for data collection and initial processing. I also acknowledge online resources on ISA and Can-Sat technology that informed this analysis, as cited above.

I thank Chaman Bhartiya School and Zero Gravity Space Labs for their contributions and mentorship.

The raw telemetry logs and processed datasets generated during the Phoenix 13 mission are openly available on Zenodo at https://zenodo.org/records/19651091. These files include high-resolution sensor readings for pressure, temperature, humidity, and 3-axis orientation.

References

1. S. Rohith, S. R. S. Prabhakar, and K. V. S. S. S.Sairam, "The Can-Sat Compendium: A Review of Scientific Can-Sats," Machines, vol. 11, no. 7, 2023.
2. International Civil Aviation Organization (ICAO), "International Standard Atmosphere (ISA)."
3. National Weather Service, "Temperature Inversions."
4. A. R. Shaik et al., "Drone-Based Vertical Atmospheric Temperature Profiling in Urban Environments," 2023.
5. Adafruit Industries, "DHT22 Temperature-Humidity Sensor."
6. Adafruit Industries, "BMP280 Barometric Pressure Sensor Datasheet."
7. L. Pandey, “Flight Telemetry and Environmental Sensor Data for Phoenix 13 CANSAT Atmospheric Probe”. Zenodo, Apr. 19, 2026.
8. L. Pandey, “A Comparative Analysis of CANSAT Flight Data and the International Standard Atmosphere in Urban Sub-Tropical Environments”. Zenodo, Apr. 17, 2026.